Ubiquity of organic nitrates from nighttime chemistry in the European submicron aerosol

DOI:
10.1002/2016GL069239

Document Version
Accepted author manuscript

Organic nitrates from night-time chemistry are ubiquitous in the European submicron aerosol

A. Kiendler-Scharr[1*], A. A. Mensah[1, #], E. Friese[2], D. Topping[3, 18], E Nemitz[4], A. S. H. Prevot[5], M. Äijälä[6], J. Allan[3, 18], F. Canonaco[5], M. Canagaratna[7], S. Carbone[8, ‡], M. Crippa[5, §], M. Dall Osto[9], D. A. Day[10], P. De Carlo[5], C.F. Di Marco[4], H. Elbern[2], A. Eriksson[11], E.Freney[12], L. Hao[13], H. Herrmann[14], L. Hildebrandt[15], R. Hillamo[8], J. L. Jimenez[10], A. Laaksonen[6,13], G. McFiggans[3], C. Mohr[5, &], C. O'Dowd[9], R. Otjes[16], J. Ovadnevaite[9], S. N. Pandis[17], L. Poulain[14], P. Schlag[1], K. Sellegri[12], E. Swietlicki[11], P. Tiitta[13], A. Vermeulen[16], A. Wahner[1], D. Worsnop[7], and H.-C. Wu[1]

[1] IEK-8: Troposphere, Forschungszentrum Jülich GmbH, Jülich, Germany
[2] Rhenish Institute for Environmental Research at the University of Cologne, Cologne, Germany
[3] School of Earth, Atmospheric and Environmental Sciences, The University of Manchester, Manchester, UK
[4] Centre for Ecology & Hydrology (CEH), Bush Estate, Penicuik, UK
[5] Paul Scherrer Institute, Villigen, Switzerland
[6] Department of Physics, Helsinki University, Helsinki, Finland
[7] Aerodyne Research Inc., Billerica, MA, USA
[8] Finnish Meteorological Institute, Helsinki, Finland
[9] National University of Ireland Galway, Galway, Ireland
[10] Cooperative Institute for Research in Environmental Sciences and Department of Chemistry and Biochemistry, University of Colorado, Boulder, CO, USA
[11]Department of Physics, Lund University, Lund, Sweden
[12] Laboratoire de Météorologie Physique, CNRS-Université Blaise Pascal, Clermont Ferrand, France
[13] Department of Applied Physics, University of Eastern Finland, Kuopio, Finland
[14] Leibniz Institute for Tropospheric Research (TROPOS), Leipzig, Germany
[15] McKetta Department of Chemical Engineering, The University of Texas at Austin, Austin, TX, USA
[16] Energy Research Centre of the Netherlands (ECN), Petten, the Netherlands
[17] Department of Chemical Engineering, University of Patras, Patras, Greece
[18] National Centre for Atmospheric Science, The University of Manchester, Manchester, UK
[#] now at: Institut f. Atmosphäre und Klima, ETH Zürich, Zürich, Switzerland
[§] now at: EC Joint Research Centre (JRC), Inst. Environment & Sustainability, Via Fermi, Ispra, Italy
[&] now at: Institute of Meteorology and Climate Research, Karlsruhe Institute of Technology, Karlsruhe, Germany
[‡] now at: IAG, University of Sao Paulo, Brasil

Corresponding author: Astrid Kiendler-Scharr (a.kiendler-scharr@fz-juelich.de)

Key Points:

- Particulate organic nitrate is ubiquitous in Europe
- 34 to 44 percent of fine particulate nitrate is organic
- Night time chemistry is a dominant source of particulate organic nitrates

Abstract

In the atmosphere night time removal of volatile organic compounds (VOC) is initiated to a large extent by reaction with the nitrate radical (NO_3) forming organic nitrates which partition between gas and particulate phase. Here we show based on particle phase measurements performed at a suburban site in the Netherlands that organic nitrates contribute substantially to particulate nitrate and organic mass. Comparisons with a chemistry transport model (CTM) indicate that most of the measured particulate organic nitrates are formed by NO_3 oxidation. Using aerosol composition data from three intensive observation periods at numerous measurement sites across Europe, we conclude that organic nitrates are a considerable fraction of fine particulate matter (PM_1) at the continental scale. Organic nitrates represent 34% to 44% of measured submicron aerosol nitrate and are found at all urban and rural sites, implying a substantial potential of PM reduction by NOx emission control.

1 Introduction

Atmospheric self-cleansing, i.e. removal of species through oxidation, is initiated by the radical species OH, O_3 and NO_3. While OH plays a key role during the day and is overall the dominant oxidant in the troposphere, NO_3 is one of the main oxidants during the night in addition to O_3. Due to its formation from the reaction of NO_2 with O_3 the main source of NO_3 is anthropogenic. Already in 1984 it was suggested that the reaction with NO_3 radicals is a dominant loss process for monoterpenes [*Winer et al.*, 1984]. Especially emissions that remain in the atmosphere at sunset or enter in the night undergo oxidation by NO_3 radicals [*Pye et al.*, 2010]. Model estimates conclude that 6-20% of the total isoprene emissions are oxidized by NO_3 [*Brown et al.*, 2009]. Oxidation of VOCs leads to either functionalization or fragmentation of precursor molecules, where fragmentation likely leads to products with higher vapour pressure than the precursors' vapour pressure. By contrast, functionalization results in a decrease of the vapour pressure [*Pankow and Asher*, 2008], which in the case of NO_3 radical reactions is dominated by addition reactions forming multifunctional nitrates ($RONO_2$). Products with low enough vapour pressures will partition to the particulate phase, forming secondary organic aerosol (SOA) and thereby contribute to air quality and climate impacts of particles.

While the formation of SOA through VOC oxidation by OH and O_3 has been studied in numerous simulation chamber and laboratory experiments [*Hallquist et al.*, 2009] only few experiments report the SOA yields from the oxidation with NO_3 (e.g. [*Boyd et al.*, 2015; *Steven S. Brown and Stutz*, 2012; *Fry et al.*, 2014]). For the biogenic VOCs investigated, SOA yields vary between 1 and 89% and $RONO_2$ yields between 19 and 66%. These reactions have also been shown to result in a substantial fraction (12 to 16%) of the oxidized nitrogen consumed by biogenic VOC oxidation in some continental regions [*Brown et al.*, 2009].

Observations of ambient atmospheric particles have shown that organic species are ubiquitous and represent a large fraction of observed mass loadings regardless of location of the measurement [*Q Zhang et al.*, 2007]. Recent attempts to model the organic aerosol (OA) mass have substantially improved the ability of models to reproduce measured organic mass loadings, yet large uncertainties remain with respect to OA sources [*Hallquist et al.*, 2009]. For instance it has been shown using radiocarbon measurements that a major part of the OA mass is of modern origin in many areas, meaning that sources such as biogenic VOC and biomass burning are often dominant sources of OA (e.g.[*Szidat et al.*, 2006]). Nevertheless SOA is often observed to correlate well with gas-phase tracers for anthropogenic activity such as carbon monoxide (CO) [*Weber et al.*, 2007], and recent model results suggest that interactions of anthropogenic pollution and biogenic VOCs (BVOCs) may be important on a global scale [*Spracklen et al.*, 2011]. A prominent candidate for production of aerosol from

modern carbon that would correlate with anthropogenic tracers is the reaction of NO_3 with BVOCs, which has been shown to serve as source of particulate organic nitrates in recent studies in the US [*Fry et al.*, 2013; *Rollins et al.*, 2012; *Setyan et al.*, 2012; *Xu et al.*, 2015a; *Xu et al.*, 2015b].
Here we present evidence from aerosol mass spectrometric (AMS) measurements with high time resolution that, in urban and rural sites in Europe, the reaction of VOCs with nitrate radicals represents an important source of OA.

2 Materials and Methods

Intensive AMS measurements were taken across Europe through three campaigns within the EUCAARI/EMEP intensives in May 2008, October 2008, and March 2009 [*Crippa et al.*, 2013; *Kulmala et al.*, 2011]. Observations were compared with results from the EURopean Air pollution and Dispersion-Inverse Model (EURAD-IM) chemistry transport model [*Elbern et al.*, 2007] in order to evaluate the regional extent of our findings. Here we discuss the data analysis principles applied to derive organic nitrate mass concentration from AMS data and the set-up of the EURAD-IM used for comparing to the measurement episodes.

2.1 AMS data analysis for organic nitrate

The working principles and modes of operation of the aerosol mass spectrometer (AMS) are described in detail elsewhere [*Canagaratna et al.*, 2007]. Here we report on the method used to quantify the organic nitrate in the measured total nitrate. In AMS measurements nitrate is primarily quantified by the determination of the total signal of NO_2^+ and NO^+ (high resolution time-of-flight version, HR-TOF-AMS [*DeCarlo et al.*, 2006]) or the signal at *m/z* 30 and *m/z* 46 that is attributed to nitrate via the so called fragmentation table (Quadrupole aerosol mass spectrometer, Q-AMS [*Jayne et al.*, 2000]). Ambiguity remains for the Q-AMS data sets due to the correction of the interference of the CH_2O^+ ion at *m/z* 30, whereas *m/z* 46 is traditionally interpreted as being dominated by NO_2^+ [*Allan et al.*, 2004]. By contrast, the HR-TOF-AMS can unambiguously distinguish between the NO^+ and CH_2O^+ ions (see Table S1 for an overview of stations and AMS type applied).

The measured ratio of NO_2^+/NO^+ was taken from all AMS data sets to determine the fractional contribution of ammonium nitrate (NH_4NO_3, hereafter $pInNO_3$) and organic nitrate ($pOrgNO_3$) to the total observed signal at these two ions. This requires knowledge of the expected ratio of NO_2^+/NO^+ for pure ammonium nitrate and pure organic nitrate. As calibrations of the ionization efficiency of the AMS are typically performed with NH_4NO_3 particles, the measured ratio of NO_2^+/NO^+ for pure NH_4NO_3 particles is known for all instruments. Table S1 in the supplement summarizes the measured calibration ratio R_{calib} of NO_2^+/NO^+ for the instruments deployed during the EUCAARI/EMEP intensive observation periods [*Crippa et al.*, 2013; *Kulmala et al.*, 2011]. Note that although there is some variability between instruments, the majority of the instruments reports calibration ratios between 0.29 and 0.49 (22 out of 25 instruments). For the remaining three data sets R_{calib} between 0.7 and 0.85 were reported. For organic nitrates literature data suggest a range of possible ratios (0.2 to 0.08) from experiments forming organic nitrates by oxidation of volatile organic compounds (VOCs) with NO_3 [*Boyd et al.*, 2015; *Bruns et al.*, 2010; *Fry et al.*, 2009; *Fry et al.*, 2011; *Rollins et al.*, 2009]. Here we use a fixed value of NO_2^+/NO^+ (i.e. 0.1) for organic nitrates (see also Figures S1 and S2 in the supplement). This number was chosen, as it represents the minimum ratio of NO_2^+/NO^+ observed in the field data sets. Note that such low ratios of NO_2^+/NO^+ were also detected in some data sets

where R_{calib} was reported high. Therefore contrary to other studies no systematic change in R_{OrgNO3} depending on R_{calib} was assumed [*Fry et al.*, 2013]. Our overall approach here is designed such that lower limits of $pOrgNO_3$ [*Xu et al.*, 2015a] are derived, with an estimated uncertainty of ± 20%.

Similar to previous attempts to determine the organic nitrate in AMS data sets [*Farmer et al.*, 2010], we apply the following formula to determine the fraction of particulate organic nitrate ($pOrgNO3_{frac}$) in the measured total nitrate from measured NO_2^+/NO^+ ratio:

$$pOrgNO3_{frac} = \frac{\left(1 + R_{OrgNO3}\right) \times \left(R_{measured} - R_{calib}\right)}{\left(1 + R_{measured}\right) \times \left(R_{OrgNO3} - R_{calib}\right)} \quad (1)$$

$$pOrgNO3_{mass} = pOrgNO3_{frac} \times NO3_{total} \quad (2)$$

Where $R_{measured}$ is the measured intensity ratio of NO_2^+ and NO^+ ions as function of time in the individual data sets, R_{calib} is the ratio observed in NH_4NO_3 calibrations, and R_{OrgNO3} is set to 0.1 for all data sets. The mass concentration of $pOrgNO_3$ ($pOrgNO3_{mass}$) is then calculated by multiplying the measured total nitrate ($NO3_{total}$) with the fraction of $pOrgNO_3$ (2). Note that since NO_2^+ is always the ion with less signal intensity, through the use of measured NO_2^+/NO^+ ratio rather than NO^+/NO_2^+ ratio, we are using a formulation that approaches zero in the case of very low or non existant signal, whereas the use of NO^+/NO_2^+ ratio gives infinite numbers as the limit of detection is approached.

Note that the pOrgNO3 calculated this way accounts for the nitrate functional group of organic nitrates only. This method was previously considered to reliably derive the $pOrgNO_3$ fraction when $pOrgNO_{3frac}$ is >0.15 [*Bruns et al.*, 2010]. Therefore organic nitrate concentration data reported here was filtered for values >0.15. Also in a conservative approach [*Bruns et al.*, 2010] we consider 0.1 µg m^{-3} $pOrgNO_3$ as detection limit and report data accordingly.

2.2 EURAD-IM Model description

The EURAD-IM, [*Elbern et al.*, 2007]) is an Eulerian model running from local to continental scale. EURAD-IM is primarily used for chemical weather forecast and advanced data assimilation studies over Europe, using the RACM chemistry mechanism [*Stockwell et al.*, 1997]. Previous studies on a high ozone episode [*Monteiro et al.*, 2012] and a dust storm [*Chervenkov and Jakobs*, 2011] indicated good performances of EURAD-IM. Within EURAD-IM, the aerosol dynamics such as nucleation, condensation, coagulation, diffusion, sedimentation, aerosol–cloud interaction, etc. are simulated by the Modal Aerosol Dynamics Model for Europe (MADE, [*Ackermann et al.*, 1998]). However, the initial MADE aerosol chemistry module only treated inorganic ions and water. To consider the formation of secondary organic aerosols, the Secondary ORGanic Aerosol Model (SORGAM) was developed and implemented into MADE [*Schell et al.*, 2001]. In SORGAM, both anthropogenic and biogenic hydrocarbons are first oxidized by oxidants like OH, NO_3 and O_3. The mass transfer from gas to particle phase is then driven by the gas/particle partitioning

of the low volatility oxidation products formed in gas phase. Aerosol dry deposition velocities are calculated according to Zhang et al. 2003 [*Zhang et al.*, 2003]. Recently it was shown that including SOA formation from NO_3 oxidation significantly improved the ability to model OOA at Cabauw, the Netherlands [*Li et al.*, 2013]. EURAD-IM is part of the MACC II consortium and, together with 6 other CTMs, operated and evaluated on a daily basis (http://www.gmes-atmosphere.eu/documents/maccii/deliverables/eva, 2013, 2013). It was found that especially NO_2 analyses performed very well.

In this study EURAD-IM was used with a spatial resolution of 15 km with improvements in the SOA scheme as described in [*Li et al.*, 2013]. Recently MEGAN 2.1 [*Guenther et al.*, 2012] has been implemented into EURAD-IM and was used for the calculation of biogenic emissions in this study. Anthropogenic emissions have been derived from the MACC-II TNO emission inventory for the year 2009 [*Pouliot et al.*, 2012]. WRF V3.5, driven by the IFS operational analysis, has been used for the provision of meteorological fields needed by EURAD-IM. The comparison of model output with measurements presented in the following focusses on SOA formed through NO_3 oxidation.

3 Organic Nitrate results from Cabauw analysis

Figure 1 shows observed mass concentrations of the submicron non-refractory aerosol species ammonium (orange), organics (green), sulphate (red), and total nitrate (blue) as measured with a HR-ToF-AMS at Cabauw, the Netherlands in May 2008 [*Mensah et al.*, 2012]. Using the observed intensity ratio of the ions NO_2^+ and NO^+ (middle panel) to calculate the relative contribution of nitrate groups associated with either $pOrgNO_3$ or $pInNO_3$ to the measured total aerosol nitrate (pNO_3), we infer a pOrgNO3 mass concentration averaging 0.52 µg m^{-3} and as high as 1.8 µg m^{-3}.

The time series of pOrgNO3 is characterized by a distinct diurnal pattern with maxima during the night (see also Figure 2) and is correlated ($R^2 = 0.58$) with the less oxidized fraction of the oxidized OA (SV-OOA), as determined by positive matrix factorization (PMF, [*Ulbrich et al.*, 2009]) and a unified ME-2 analysis for all EUCAARI/EMEP data sets [*Crippa et al.*, 2013; *Paglione et al.*, 2014]. Note that this correlation between pOrgNO3 and SV-OOA is more pronounced than the correlation of total pNO3 with SV-OOA.

It has to be emphasized, that pOrgNO3 measures the nitrate functionality of organic nitrates only. To account for the total particulate organic nitrate mass ($RONO_2$), an estimate needs to be made regarding the molar mass of $RONO_2$ relative to molar mass of NO_3. As a lower limit we will assume a molar mass of 200 g mol^{-1} in calculations of the contribution of organic nitrates to total organics [*Xu et al.*, 2015a; *Lee et al.*, 2016].

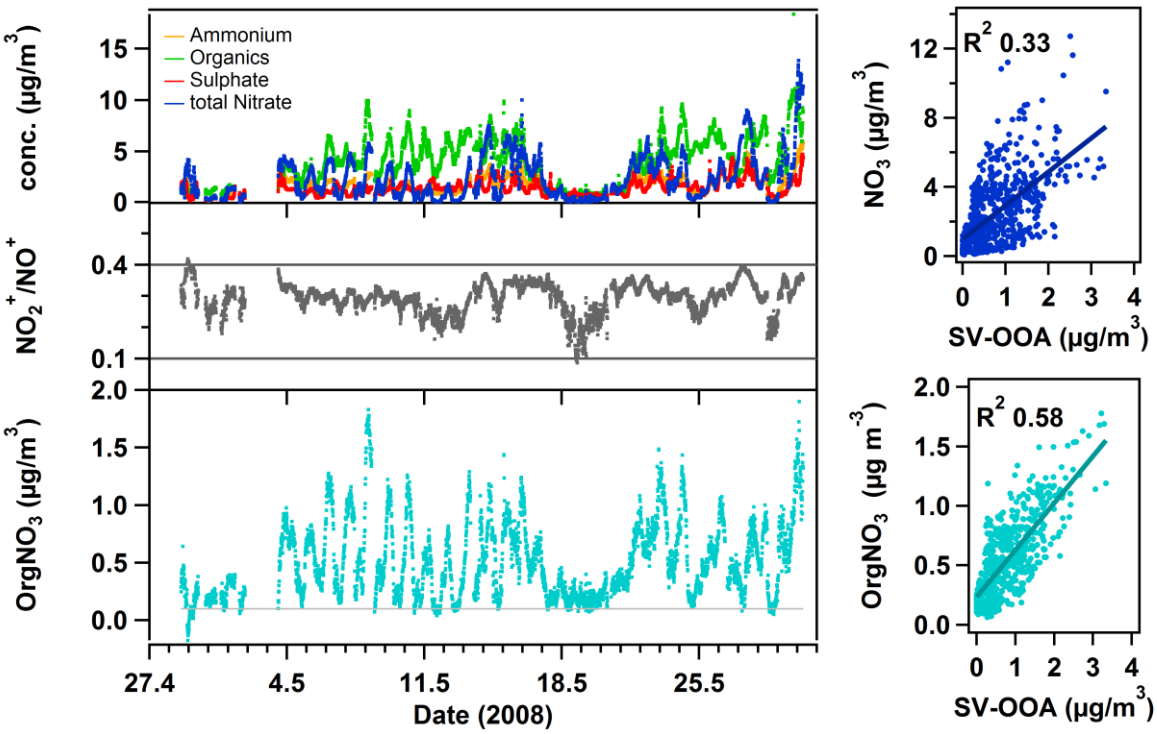

Figure 1. Measured mass concentrations of ammonium (orange), total nitrate (dark blue), sulphate (red) and organics (green) together with observed concentration ratio of NO_2^+/NO^+ ions (dark grey) and organic nitrate ($pOrgNO_3$, cyan) mass concentration at Cabauw, the Netherlands. Also shown are correlations of the SV-OOA factor with total nitrate (top right) and organic nitrate (bottom right).

Using the EURAD-IM model, the SOA formed from oxidation of VOCs by NO_3 was modelled for the measurement period of May 2008 at Cabauw [*Li et al.*, 2013]. As shown in Figure 2, the temporal behaviour of the modelled SOA from NO_3 oxidation closely matches the observed SV-OOA and $pOrgNO_3$ time series. Maximum concentrations are observed for all three at 5:00 LT with a daytime minimum extending from 10:00 to 20:00 LT. For comparison, radon concentration, which can be considered as a tracer for boundary layer dilution, is observed to have a maximum between 7:00 and 8:00 LT i.e. later than $pOrgNO_3$. This is in agreement with a modelled time lag of 2 hours between the early morning decrease of SOA from NO_3 oxidation (due to NO_3 photolysis and thus halted production) and the decrease of a dilution tracer (due to break-up of the nocturnal boundary layer) in the EURAD-IM model. Together with a distinct daytime maximum of the photo-chemically formed sulphate (see Figure S3), we take this comparison as further support that the observed organic nitrate is primarily formed through night time NO_3 chemistry.

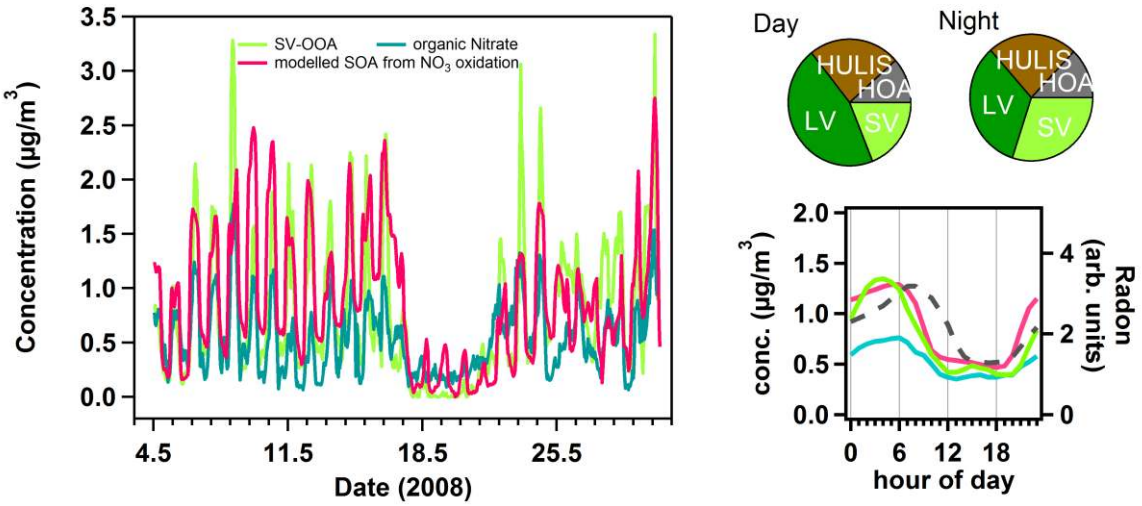

Figure 2. Time series of the mass concentrations of measured organic nitrate and SV-OOA, and modelled SOA from NO_3 oxidation at Cabauw during May 2008. Inserts show the average diurnal including also Radon concentration (grey dashed line, right axis) as boundary layer dilution tracer, and day and night pie charts of the relative contribution of individual organic PMF factors.

4 Organic Nitrate across Europe

Extending the data analysis to the full EUCAARI/EMEP AMS data set [*Kulmala et al.*, 2011] we find that $pOrgNO_3$ is present throughout Europe (Figure 3) with observed concentrations likely a result of complex interplay of various sources and sinks. Maximum concentrations of $pOrgNO_3$ are observed for European sites with large anthropogenic influence, i.e. urban (2 sites) and rural (9 sites) environments, whereas $pOrgNO_3$ is very low or below detection limit at the three remote and two high altitude sites. Averaging over all stations, the fraction of aerosol nitrate that is observed to be $pOrgNO_3$ showed little variability with values of 34%, 38% and 44% in March 2009, May 2008, and October 2008, respectively (see Tables S1 and S2 in Supplement for details [*Carbone et al.*, 2014; *Dall'Osto et al.*, 2010; *Freney et al.*, 2011; *Hildebrandt et al.*, 2011; *Lanz et al.*, 2010; *Mensah et al.*, 2012; *Minguillón et al.*, 2011; *Mohr et al.*, 2012; *Paglione et al.*, 2014; *Pikridas et al.*, 2010; *Poulain et al.*, 2011; *Saarikoski et al.*, 2012]). Assuming a molar mass of 200 g mol^{-1} for organic nitrates, the mean fractional contribution of organic nitrates to organics was 46% for stations fulfilling the threshold criterion of pOrgNO3 > 0.1 µg m^{-3} (18 out of 25 data sets). Note that this is equivalent to a contribution of organic nitrates to non-refractory PM1 of between 5.6 and 51% (average 22%).

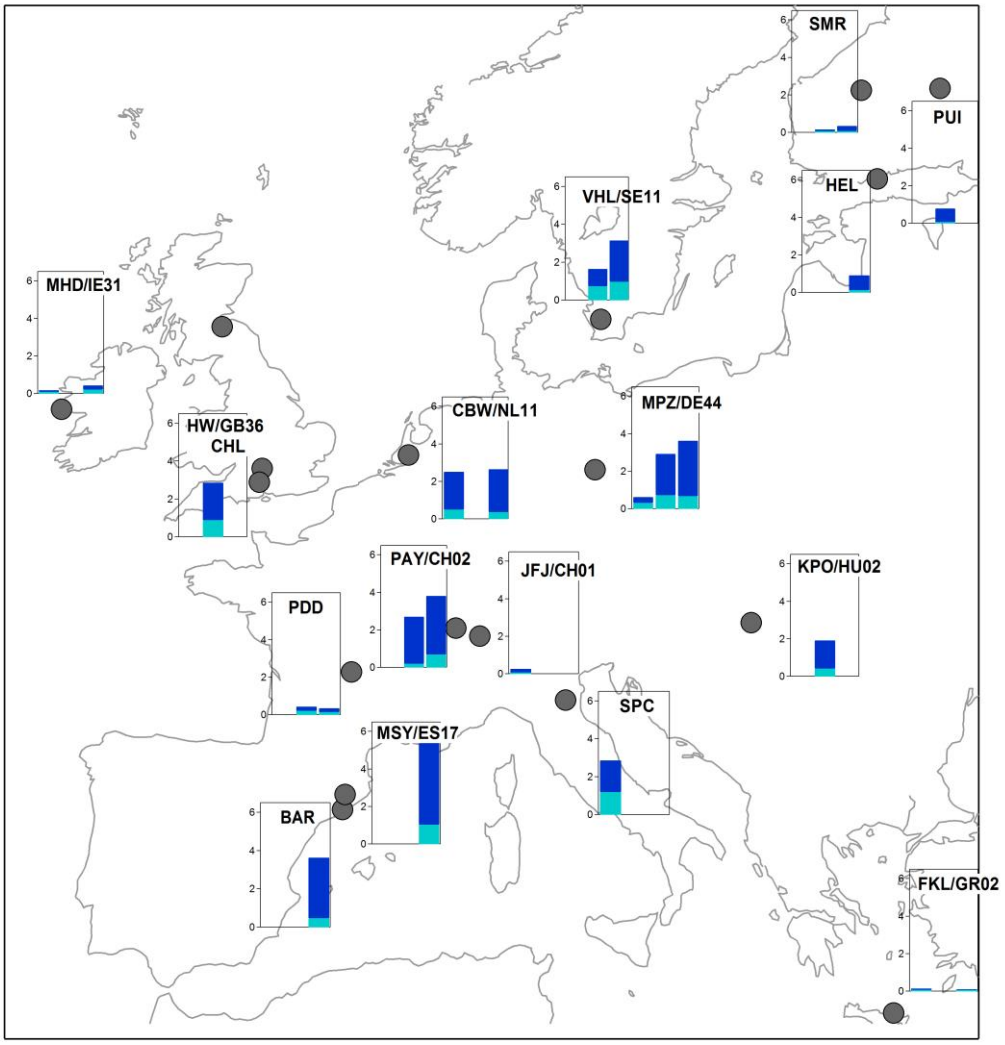

Figure 3. Map overview of particulate inorganic nitrate ($pInNO_3$, dark blue) and particulate organic nitrate ($pOrgNO_3$, cyan) mass concentrations (µg m^{-3}) as observed during the EUCAARI EMEP intensive measurement periods in May 2008 (left bar), October 2008 (middle), and March 2009 (right). Organic nitrate mass concentrations are high in all urban and rural sites and reach maximum concentrations during the night (see supplement for detailed time series plots, diurnals, and station abbreviations).

Measurements of $RONO_2$ in ambient aerosol have so far mainly been performed from filter samples and therefore with low time resolution. Detection of $RONO_2$ is usually achieved via detection of the $-ONO_2$ group either optically or by mass spectrometry, with recent developments made towards high time resolution detection of RONO2 [*Ayres et al.*, 2015; *Hao et al.*, 2014; *Rollins et al.*, 2012; *Schlag et al.*, 2015; *Sun et al.*, 2012; *Xu et al.*, 2015a; *Xu et al.*, 2015b]. Comparing with literature data obtained mainly from offline and online aerosol analysis in individual case studies in the US and Europe [*Brown and Stutz*, 2012; *Fry et al.*, 2013; *Rollins et al.*, 2012; *Setyan et al.*, 2012; *Xu et al.*, 2015a; *Xu et al.*, 2015b] we find a high contribution of organic nitrates to total organic PM1. For example recent analysis of data from the south east US find that organic nitrates contribute 5 to 12 percent to organic aerosol in summer [*Xu et al.*, 2015a; *Xu et al.*, 2015b], whereas the results here imply a contribution of organic nitrates to European PM1 organics of on average 46 percent.

Exploiting the high time resolution of AMS measurements, for the first time it is shown in an extended data set (spanning a continent and multiple seasons) that the concentration of organic nitrate is maximum during the night time for 12 of the 19 data sets with pOrgNO3 above detection limit (see Figures S4 – S7). Recent modelling studies suggest that at the global scale, 13% of the biogenic SOA production originates from NO_3 oxidation [*Pye et al.*, 2010]. For summer time in the USA up to 3.35 µg m^{-3} of SOA is formed from NO_3 oxidation of biogenic VOC, equivalent to a doubling of the terpene SOA in some regions, when considering the formation by NO_3 oxidation [*Pye et al.*, 2010]. Similarly our simulations for Europe (details see supplement) show an increase of SOA by 50 to 70% when considering SOA formation by NO_3 oxidation with maximum ground level concentrations of SOA from NO_3 oxidation in the range of 2 to 4 µg m^{-3} in May 2008 (Figure 4).

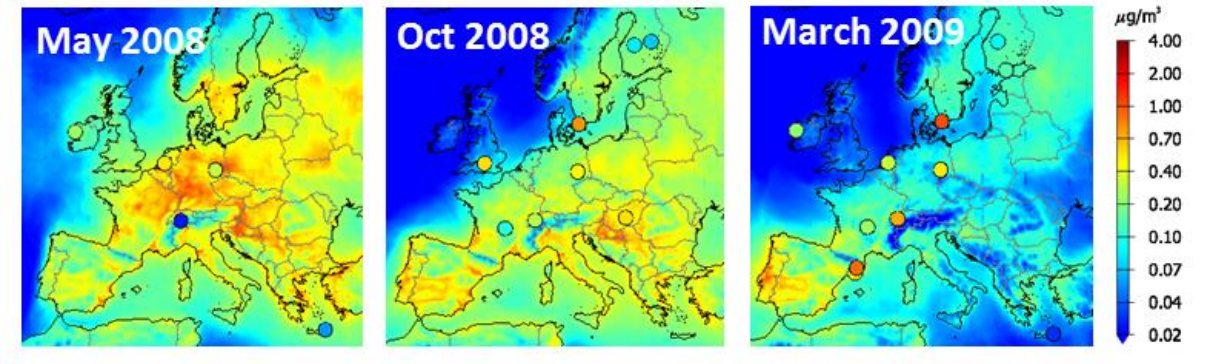

Figure 4. EURAD monthly mean concentration fields for SOA from NO_3 oxidation together with observed concentrations of $pOrgNO_3$ (coloured circles) for May 2008 (left), October 2008 (middle), and March 2009 (right), respectively.

As shown in Figure S8 and summarized in Table S3, EURAD-IM performed well in predicting organic PM_1 concentrations with an overall normalized mean error (NME) of 53% and a normalized mean bias (NMB) of -45%. It reproduces observed daily mean organic aerosol concentration within a factor of ten for 98% of all data points and within a factor of two for 57% of all data points. On the other hand, EURAD underestimates SOA from NO_3 when compared with observed pOrgNO3 with a normalized mean bias (NMB) of -50% and an overall normalized mean error (NME) of 85%. This is worth mentioning specifically since $pOrgNO_3$ as measured here represents only a small fraction of SOA from NO_3 for two reasons. First the $pOrgNO_3$ concentration reported is measure of the mass concentration of the nitrate functionality only of $RONO_2$. Second the reaction of VOC with NO_3 also leads to the formation of products without NO_3 functionality, therefore not covered in the measurement assignment of $pOrgNO_3$ to SOA from NO_3 oxidation. This under estimation is likely due to overall uncertainties in the modeling of SOA. The model treats NO_3 oxidation of anthropogenic VOCs (Cresole and other hydroxy substituted aromatics, terminal and internal alkenes) and biogenic VOCs (isoprene, a-pinene and other cyclic terpenes with one double bond, d-limonene and other cyclic diene-terpenes) according to the RACM [*Stockwell et al.*, 1997] chemistry mechanism. First and foremost, emission strengths of these VOCs are highly uncertain. Especially the estimation of biogenic VOC emissions is critical due to a lack of detailed information about the type of plant cover. Further uncertainties may be introduced by the lumping applied to chemical species in the RACM chemistry mechanism and by the simplifying assumption that SOA formation from NO_3 oxidation for all biogenic VOC can be parameterized according to results obtained from α-pinene, limonene, and isoprene [*Li et al.*, 2013]. This assumption is a consequence of the limited number of experimental studies

available. It should also be mentioned that the comparison shows a larger NMB for the March 2009 data set (-74%) potentially indicating the presence of additional sources of pOrgNO3 beyond oxidation of VOC with NO_3. Due to the coarse model resolution (15 km) some of the measurement sites are not representative for the grid box used for comparison. Especially a comparison of measurement data and model results is highly uncertain for the stations Jungfraujoch and Puy de Dome because of their exposed position. Also in particular the $pOrgNO_3$ measured at Vavihill, a continental background site with no local sources of pollution, situated in the southern-most part of Sweden, greatly exceeds modelled SOA from NO_3 (see also Figure 4). This potentially hints at additional sources for $pOrgNO_3$ at the Vavihill measurement site, potentially through influx of polluted air from continental Europe to the Nordic countries along a south-north transect. The inversion algorithm of EURAD-IM is currently designed as an inversion algorithm for gas phase [*Elbern et al.*, 2007]. Once the adjoint of SORGAM is available it will be extended for SOA precursor emission estimation, Based on MODIS land use information, and higher horizontal resolution, the deficits can be addressed in a more systematic way. Furthermore, SORGAM improvements are expected taking recent experimental results on SOA formation due to reaction of a-pinene and b-pinene with NO_3 into account [*Boyd et al.*, 2015; *Nah et al.*, 2016; *Xu et al.*, 2015a; *Xu et al.*, 2015b]. Disregarding the underestimation of daily mean pOrgNO3 concentrations at some measurement sites, the ability of the EURAD-IM to demonstrate qualitatively the daily cycle of pOrgNO3 and the dilution tracer radon, supports the assumption that nighttime NO_3 chemistry contributes significantly to the pOrgNO3 production.

The spatial distribution and diurnal pattern of $pOrgNO_3$ indicate a gradient of concentration with high concentration found in source regions, i.e. regions with high NO_x emissions and during night time, and low concentrations in remote regions and during the day. Part of the diurnal pattern will be due to boundary layer dynamics, but the question remains to what extent the observed diurnal and regional variability is indicative of deposition losses, chemical reactions leading to fragmentation, or evaporative loss.

5 Implications and Conclusions

Across Europe a large fraction of the AMS measured nitrate is found to be organic, emphasizing the need to better understand sources and properties of particulate organic nitrates. The modelled continental distribution of SOA from NO_3 by the EURAD-IM supports the importance of NO_3 reactions during the night leading to SOA in regions with high NOx emissions. It also shows the need for more extensive investigations of the chemistry and emissions leading to $pOrgNO_3$.

Due to the lifetime of gas-phase $RONO_2$ with respect to photolysis (12-20 days), OH reactions (3-40 days), or thermal decomposition (up to months), some $RONO_2$ molecules may represent a temporary NO_x reservoir [*Aschmann et al.*, 2011; *Brown and Stutz*, 2012; *Nah et al.*, 2016]; whereas, other organic molecules may be lost rapidly due to gas-phase deposition [*Farmer et al.*, 2006; *Lee et al.*, 2016] or particle phase hydrolysis [*Boyd et al.*, 2015; *Liu et al.*, 2012]. Particulate $RONO_2$ could serve as source of NO_x in regions without major anthropogenic NO_x sources due to repartitioning of organic nitrates [*Fry et al.*, 2013] into the gas phase or release of NO_x following heterogeneous reactions [*Liu et al.*, 2012]. On the other hand recent laboratory-based observations indicate that $RONO_2$ might irreversibly condense on SOA [*Perraud et al.*, 2012]. This would imply that particulate $RONO_2$ can serve as an important NO_x sink.

Little is known about the properties of particulate organic nitrate with respect to both health risks and climate effects. Direct climate effects of organic nitrates may arise from their absorbing properties, which could be significantly higher than for SOA formed from OH or O3 initiated oxidation [*Moise et al.*, 2015]. Similar to other organic semi-volatile vapours, organic nitrates can be expected to co-condense with water when aerosol particles activate to cloud droplets [*Topping et al.*, 2013], impacting aerosol indirect effects on climate. At the median level, for all sites studied here organic nitrates suggest a comparable contribution to increasing kappa as nitric acid (see Supplement and Figure S9 [*Barley et al.*, 2011; *Topping and McFiggans*, 2012]). Such effects of organic nitrate condensation onto activating aerosol particles should be considered alongside those from nitric acid in increasing the number concentration of cloud droplets. Through its formation by NO_3 oxidation, and thereby its strong relation to anthropogenic NO_x emissions, particulate organic nitrates will be directly affected by NO_x emission controls [*Rollins et al.*, 2012] with the potential to decrease specifically night time PM_1 burdens in urban and rural sites in Europe.

Acknowledgments and Data

This work was supported by the European Commission through EUCAARI IP (contract no. 036833-2) and PEGASOS (FP7-ENV-2010-265148). Transnational access to the measurement sites in Cabauw and Kpuszta was supported by ACCENT. Measurements were further funded by the following national sources: the UK Department for Environment, Food and Rural Affairs (Defra), the German Federal Environment Agency (Umweltbundesamt, grants No. 351 03 031 and 351 01 038, and UFOPLAN grant 3703 43 200), the Swiss Federal Office for the Environment, and NOAA NA13OAR4310063 & EPA STAR 83587701-0.

References

Ackermann, I. J., H. Hass, M. Memmesheimer, A. Ebel, F. S. Binkowski, and U. Shankar (1998), Modal aerosol dynamics model for Europe: Development and first applications, *Atmospheric Environment*, *32*(17), 2981-2999.

Allan, J. D., et al. (2004), A generalised method for the extraction of chemically resolved mass spectra from aerodyne aerosol mass spectrometer data, *Journal of Aerosol Science*, *35*(7), 909-922.

Aschmann, S. M., E. C. Tuazon, J. Arey, and R. Atkinson (2011), Products of the OH radical-initiated reactions of 2-propyl nitrate, 3-methyl-2-butyl nitrate and 3-methyl-2-pentyl nitrate, *Atmospheric Environment*, *45*(9), 1695-1701.

Ayres, B. R., et al. (2015), Organic nitrate aerosol formation via NO₃ + biogenic volatile organic compounds in the southeastern United States, *Atmos. Chem. Phys.*, *15*(23), 13377-13392.

Barley, M. H., D. Topping, D. Lowe, S. Utembe, and G. McFiggans (2011), The sensitivity of secondary organic aerosol (SOA) component partitioning to the predictions of component properties – Part 3: Investigation of condensed compounds generated by a near-explicit model of VOC oxidation, *Atmos. Chem. Phys.*, *11*(24), 13145-13159.

Boyd, C. M., J. Sanchez, L. Xu, A. J. Eugene, T. Nah, W. Y. Tuet, M. I. Guzman, and N. L. Ng (2015), Secondary organic aerosol formation from the β-pinene+NO₃ system: effect of humidity and peroxy radical fate, *Atmos. Chem. Phys.*, *15*(13), 7497-7522.

Brown, S. S., and J. Stutz (2012), Nighttime radical observations and chemistry, *Chemical Society Reviews*, *41*(19), 6405-6447.

Brown, S. S., et al. (2009), Nocturnal isoprene oxidation over the Northeast United States in summer and its impact on reactive nitrogen partitioning and secondary organic aerosol, *Atmos. Chem. Phys.*, *9*(9), 3027-3042.

Bruns, E. A., V. r. Perraud, A. Zelenyuk, M. J. Ezell, S. N. Johnson, Y. Yu, D. Imre, B. J. Finlayson-Pitts, and M. L. Alexander (2010), Comparison of FTIR and Particle Mass Spectrometry for the Measurement of Particulate Organic Nitrates, *Environmental Science & Technology*, *44*(3), 1056-1061.

Canagaratna, M. R., et al. (2007), Chemical and microphysical characterization of ambient aerosols with the aerodyne aerosol mass spectrometer, *Mass Spectrometry Reviews*, *26*(2), 185-222.

Carbone, S., et al. (2014), Wintertime Aerosol Chemistry in Sub-Arctic Urban Air, *Aerosol Science and Technology*, *48*(3), 313-323.
Chervenkov, H., and H. Jakobs (2011), Dust storm simulation with regional air quality model - Problems and results, *Atmospheric Environment*, *45*(24), 3965-3976.
Crippa, M., et al. (2013), Organic aerosol components derived from 25 AMS datasets across Europe using a newly developed ME-2 based source apportionment strategy, *Atmos. Chem. Phys. Discuss.*, *13*(9), 23325-23371.
Dall'Osto, M., et al. (2010), Aerosol properties associated with air masses arriving into the North East Atlantic during the 2008 Mace Head EUCAARI intensive observing period: an overview, *Atmos. Chem. Phys.*, *10*(17), 8413-8435.
DeCarlo, P. F., et al. (2006), Field-Deployable, High-Resolution, Time-of-Flight Aerosol Mass Spectrometer, *Anal. Chem.*, *78*(24), 8281–8289.
Elbern, H., A. Strunk, H. Schmidt, and O. Talagrand (2007), Emission rate and chemical state estimation by 4-dimensional variational inversion, *Atmospheric Chemistry and Physics*, *7*(14), 3749-3769.
Farmer, D. K., P. J. Wooldridge, and R. C. Cohen (2006), Application of thermal-dissociation laser induced fluorescence (TD-LIF) to measurement of HNO3, Σalkyl nitrates, Σperoxy nitrates, and NO2 fluxes using eddy covariance, *Atmos. Chem. Phys.*, *6*(11), 3471-3486.
Farmer, D. K., A. Matsunaga, K. S. Docherty, J. D. Surratt, J. H. Seinfeld, P. J. Ziemann, and J. L. Jimenez (2010), Response of an aerosol mass spectrometer to organonitrates and organosulfates and implications for atmospheric chemistry, *Proceedings of the National Academy of Sciences*, *107*(15), 6670-6675.
Freney, E. J., K. Sellegri, F. Canonaco, J. Boulon, M. Hervo, R. Weigel, J. M. Pichon, A. Colomb, A. S. H. Prévôt, and P. Laj (2011), Seasonal variations in aerosol particle composition at the puy-de-Dôme research station in France, *Atmos. Chem. Phys.*, *11*(24), 13047-13059.
Fry, J. L., et al. (2014), Secondary Organic Aerosol Formation and Organic Nitrate Yield from NO3 Oxidation of Biogenic Hydrocarbons, *Environmental Science & Technology*, *48*(20), 11944-11953.
Fry, J. L., et al. (2009), Organic nitrate and secondary organic aerosol yield from NO3 oxidation of Î²-pinene evaluated using a gas-phase kinetics/aerosol partitioning model, *Atmos. Chem. Phys.*, *9*(4), 1431-1449.
Fry, J. L., et al. (2011), SOA from limonene: role of NO(3) in its generation and degradation, *Atmospheric Chemistry and Physics*, *11*(8), 3879-3894.
Fry, J. L., et al. (2013), Observations of gas- and aerosol-phase organic nitrates at BEACHON-RoMBAS 2011, *Atmos. Chem. Phys.*, *13*(17), 8585-8605.
Guenther, A. B., X. Jiang, C. L. Heald, T. Sakulyanontvittaya, T. Duhl, L. K. Emmons, and X. Wang (2012), The Model of Emissions of Gases and Aerosols from Nature version 2.1 (MEGAN2.1): an extended and updated framework for modeling biogenic emissions, *Geoscientific Model Development*, *5*(6), 1471-1492.
Hallquist, M., et al. (2009), The formation, properties and impact of secondary organic aerosol: current and emerging issues, *Atmospheric Chemistry and Physics*, *9*(14), 5155-5236.
Hao, L. Q., et al. (2014), Atmospheric submicron aerosol composition and particulate organic nitrate formation in a boreal forestland–urban mixed region, *Atmos. Chem. Phys.*, *14*(24), 13483-13495.
Hildebrandt, L., E. Kostenidou, V. A. Lanz, A. S. H. Prevot, U. Baltensperger, N. Mihalopoulos, A. Laaksonen, N. M. Donahue, and S. N. Pandis (2011), Sources and atmospheric processing of organic aerosol in the Mediterranean: insights from aerosol mass spectrometer factor analysis, *Atmos. Chem. Phys.*, *11*(23), 12499-12515.
Jayne, J. T., D. C. Leard, X. F. Zhang, P. Davidovits, K. A. Smith, C. E. Kolb, and D. R. Worsnop (2000), Development of an aerosol mass spectrometer for size and composition analysis of submicron particles, *Aerosol Science and Technology*, *33*(1-2), 49-70.
Kulmala, M., et al. (2011), General overview: European Integrated project on Aerosol Cloud Climate and Air Quality interactions (EUCAARI) – integrating aerosol research from nano to global scales, *Atmos. Chem. Phys.*, *11*(24), 13061-13143.
Lanz, V. A., et al. (2010), Characterization of aerosol chemical composition with aerosol mass spectrometry in Central Europe: an overview, *Atmos. Chem. Phys.*, *10*(21), 10453-10471.
Lee, B. H., et al. (2016), Highly functionalized organic nitrates in the southeast United States: Contribution to secondary organic aerosol and reactive nitrogen budgets, *Proceedings of the National Academy of Sciences*, *113*(6), 1516-1521.
Li, Y. P., H. Elbern, K. D. Lu, E. Friese, A. Kiendler-Scharr, T. F. Mentel, X. S. Wang, A. Wahner, and Y. H. Zhang (2013), Updated aerosol module and its application to simulate secondary organic aerosols during IMPACT campaign May 2008, *Atmospheric Chemistry and Physics*, *13*(13), 6289-6304.
Liu, S., J. E. Shilling, C. Song, N. Hiranuma, R. A. Zaveri, and L. M. Russell (2012), Hydrolysis of Organonitrate Functional Groups in Aerosol Particles, *Aerosol Science and Technology*, *46*(12), 1359-1369.
Mensah, A. A., R. Holzinger, R. Otjes, A. Trimborn, T. F. Mentel, H. ten Brink, B. Henzing, and A. Kiendler-Scharr (2012), Aerosol chemical composition at Cabauw, The Netherlands as observed in two intensive periods in May 2008 and March 2009, *Atmos. Chem. Phys.*, *12*(10), 4723-4742.
Minguillón, M. C., et al. (2011), Fossil versus contemporary sources of fine elemental and organic carbonaceous particulate matter during the DAURE campaign in Northeast Spain, *Atmos. Chem. Phys.*, *11*(23), 12067-12084.

Mohr, C., et al. (2012), Identification and quantification of organic aerosol from cooking and other sources in Barcelona using aerosol mass spectrometer data, *Atmos. Chem. Phys.*, *12*(4), 1649-1665.
Moise, T., J. M. Flores, and Y. Rudich (2015), Optical Properties of Secondary Organic Aerosols and Their Changes by Chemical Processes, *Chemical Reviews*, *115*(10), 4400-4439.
Monteiro, A., et al. (2012), Investigating a high ozone episode in a rural mountain site, *Environmental Pollution*, *162*, 176-189.
Nah, T., J. Sanchez, C. M. Boyd, and N. L. Ng (2016), Photochemical Aging of α-pinene and β-pinene Secondary Organic Aerosol formed from Nitrate Radical Oxidation, *Environmental Science & Technology*, *50*(1), 222-231.
Paglione, M., et al. (2014), Identification of humic-like substances (HULIS) in oxygenated organic aerosols using NMR and AMS factor analyses and liquid chromatographic techniques, *Atmos. Chem. Phys.*, *14*(1), 25-45.
Pankow, J. F., and W. E. Asher (2008), SIMPOL.1: a simple group contribution method for predicting vapor pressures and enthalpies of vaporization of multifunctional organic compounds, *Atmos. Chem. Phys.*, *8*(10), 2773-2796.
Perraud, V., et al. (2012), Nonequilibrium atmospheric secondary organic aerosol formation and growth, *Proceedings of the National Academy of Sciences*, *109*(8), 2836-2841.
Pikridas, M., et al. (2010), The Finokalia Aerosol Measurement Experiment – 2008 (FAME-08): an overview, *Atmos. Chem. Phys.*, *10*(14), 6793-6806.
Poulain, L., G. Spindler, W. Birmili, C. Plass-Dülmer, A. Wiedensohler, and H. Herrmann (2011), Seasonal and diurnal variations of particulate nitrate and organic matter at the IfT research station Melpitz, *Atmos. Chem. Phys.*, *11*(24), 12579-12599.
Pouliot, G., T. Pierce, H. D. van der Gon, M. Schaap, M. Moran, and U. Nopmongcol (2012), Comparing emission inventories and model-ready emission datasets between Europe and North America for the AQMEII project, *Atmospheric Environment*, *53*, 4-14.
Pye, H. O. T., A. W. H. Chan, M. P. Barkley, and J. H. Seinfeld (2010), Global modeling of organic aerosol: the importance of reactive nitrogen (NOx and NO3), *Atmos. Chem. Phys.*, *10*(22), 11261-11276.
Rollins, A. W., et al. (2012), Evidence for NOx Control over Nighttime SOA Formation, *Science*, *337*(6099), 1210-1212.
Rollins, A. W., et al. (2009), Isoprene oxidation by nitrate radical: alkyl nitrate and secondary organic aerosol yields, *Atmos. Chem. Phys.*, *9*(18), 6685-6703.
Saarikoski, S., et al. (2012), Chemical characterization of springtime submicrometer aerosol in Po Valley, Italy, *Atmos. Chem. Phys. Discuss.*, *12*(3), 8269-8318.
Schell, B., I. J. Ackermann, H. Hass, F. S. Binkowski, and A. Ebel (2001), Modeling the formation of secondary organic aerosol within a comprehensive air quality model system, *J. Geophys. Res.-Atmos.*, *106*(D22), 28275-28293.
Schlag, P., A. Kiendler-Scharr, M. J. Blom, F. Canonaco, J. S. Henzing, M. M. Moerman, A. S. H. Prévôt, and R. Holzinger (2015), Aerosol source apportionment from 1 year measurements at the CESAR tower at Cabauw, NL, *Atmos. Chem. Phys. Discuss.*, *2015*, 35117-35155.
Setyan, A., et al. (2012), Characterization of submicron particles influenced by mixed biogenic and anthropogenic emissions using high-resolution aerosol mass spectrometry: results from CARES, *Atmos. Chem. Phys.*, *12*(17), 8131-8156.
Spracklen, D. V., et al. (2011), Aerosol mass spectrometer constraint on the global secondary organic aerosol budget, *Atmos. Chem. Phys.*, *11*(23), 12109-12136.
Stockwell, W. R., F. Kirchner, M. Kuhn, and S. Seefeld (1997), A new mechanism for regional atmospheric chemistry modeling, *Journal of Geophysical Research: Atmospheres*, *102*(D22), 25847-25879.
Sun, Y. L., Q. Zhang, J. J. Schwab, T. Yang, N. L. Ng, and K. L. Demerjian (2012), Factor analysis of combined organic and inorganic aerosol mass spectra from high resolution aerosol mass spectrometer measurements, *Atmos. Chem. Phys.*, *12*(18), 8537-8551.
Szidat, S., T. M. Jenk, H.-A. Synal, M. Kalberer, L. Wacker, I. Hajdas, A. Kasper-Giebl, and U. Baltensperger (2006), Contributions of fossil fuel, biomass-burning, and biogenic emissions to carbonaceous aerosols in Zurich as traced by 14C, *J. Geophys. Res.*, *111*(D7), D07206.
Topping, D., P. Connolly, and G. McFiggans (2013), Cloud droplet number enhanced by co-condensation of organic vapours, *Nat. Geosci.*, *6*(6), 443-446.
Topping, D. O., and G. McFiggans (2012), Tight coupling of particle size, number and composition in atmospheric cloud droplet activation, *Atmos. Chem. Phys.*, *12*(7), 3253-3260.
Ulbrich, I. M., M. R. Canagaratna, Q. Zhang, D. R. Worsnop, and J. L. Jimenez (2009), Interpretation of organic components from Positive Matrix Factorization of aerosol mass spectrometric data, *Atmos. Chem. Phys.*, *9*(9), 2891-2918.
Weber, R. J., et al. (2007), A study of secondary organic aerosol formation in the anthropogenic-influenced southeastern United States, *J. Geophys. Res.-Atmos.*, *112*(D13).
Winer, A. M., R. Atkinson, and J. N. Pitts (1984), Gaseous Nitrate Radical: Possible Nighttime Atmospheric Sink for Biogenic Organic Compounds, *Science*, *224*(4645), 156-159.

Xu, L., S. Suresh, H. Guo, R. J. Weber, and N. L. Ng (2015a), Aerosol characterization over the southeastern United States using high-resolution aerosol mass spectrometry: spatial and seasonal variation of aerosol composition and sources with a focus on organic nitrates, *Atmos. Chem. Phys.*, *15*(13), 7307-7336.
Xu, L., et al. (2015b), Effects of anthropogenic emissions on aerosol formation from isoprene and monoterpenes in the southeastern United States, *Proceedings of the National Academy of Sciences*, *112*(1), 37-42.
Zhang, L., J. R. Brook, and R. Vet (2003), A revised parameterization for gaseous dry deposition in air-quality models, *Atmos. Chem. Phys.*, *3*(6), 2067-2082.
Zhang, Q., et al. (2007), Ubiquity and dominance of oxygenated species in organic aerosols in anthropogenically-influenced Northern Hemisphere midlatitudes, *Geophysical Research Letters*, *34*(13).

Figure 1. Figure

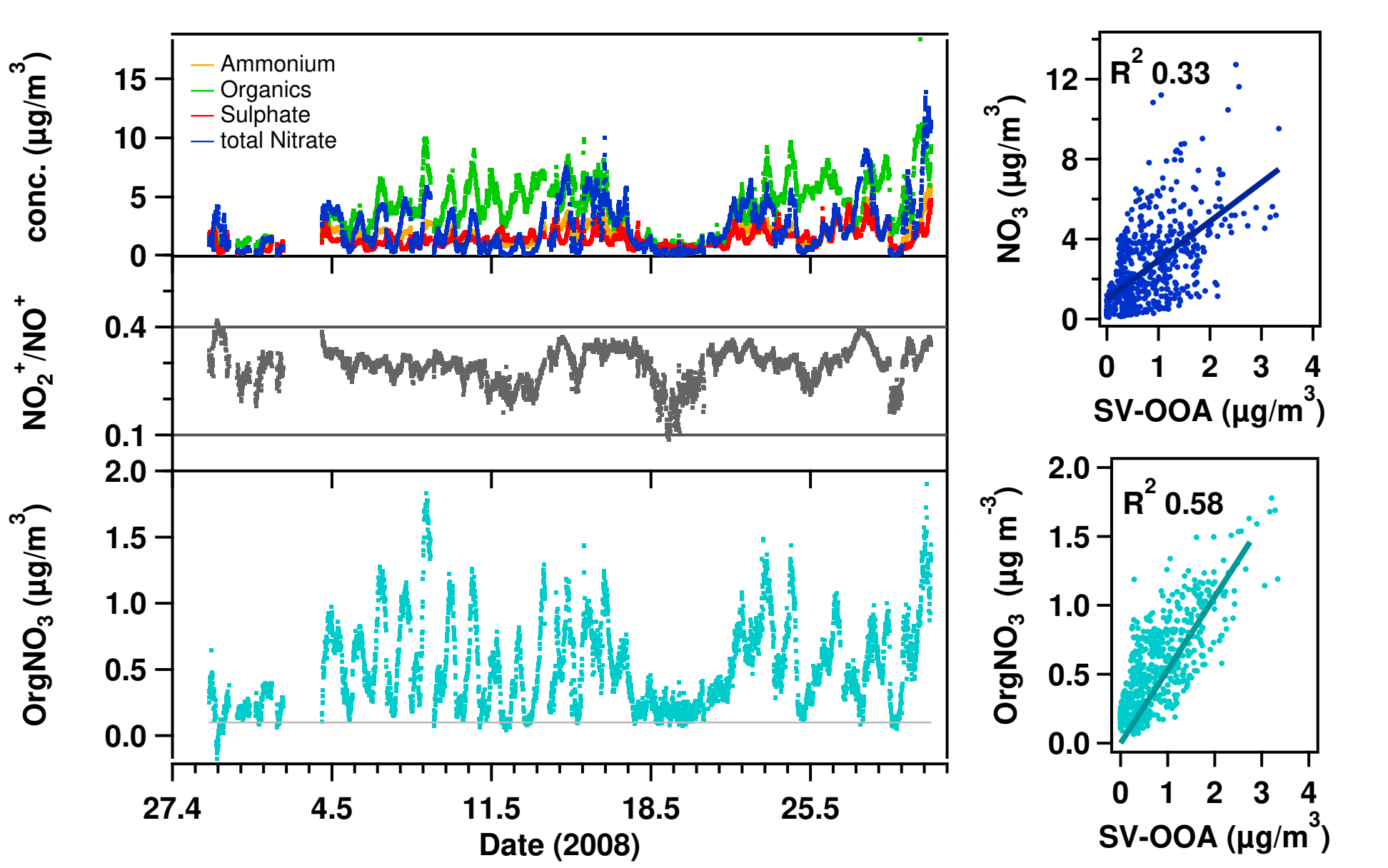
Ammonium
Organics
Sulphate
total Nitrate
conc. (µg/m3)
15
10
5
0
NO2+/NO+
0.4
0.1
2.0
OrgNO3 (µg/m3)
1.5
1.0
0.5
0.0
27.4
4.5
11.5
18.5
25.5
Date (2008)
R2 0.33
NO3 (µg/m3)
12
8
4
0
0 1 2 3 4
SV-OOA (µg/m3)
R2 0.58
OrgNO3 (µg m-3)
2.0
1.5
1.0
0.5
0.0
0 1 2 3 4
SV-OOA (µg/m3)

Figure 2. Figure

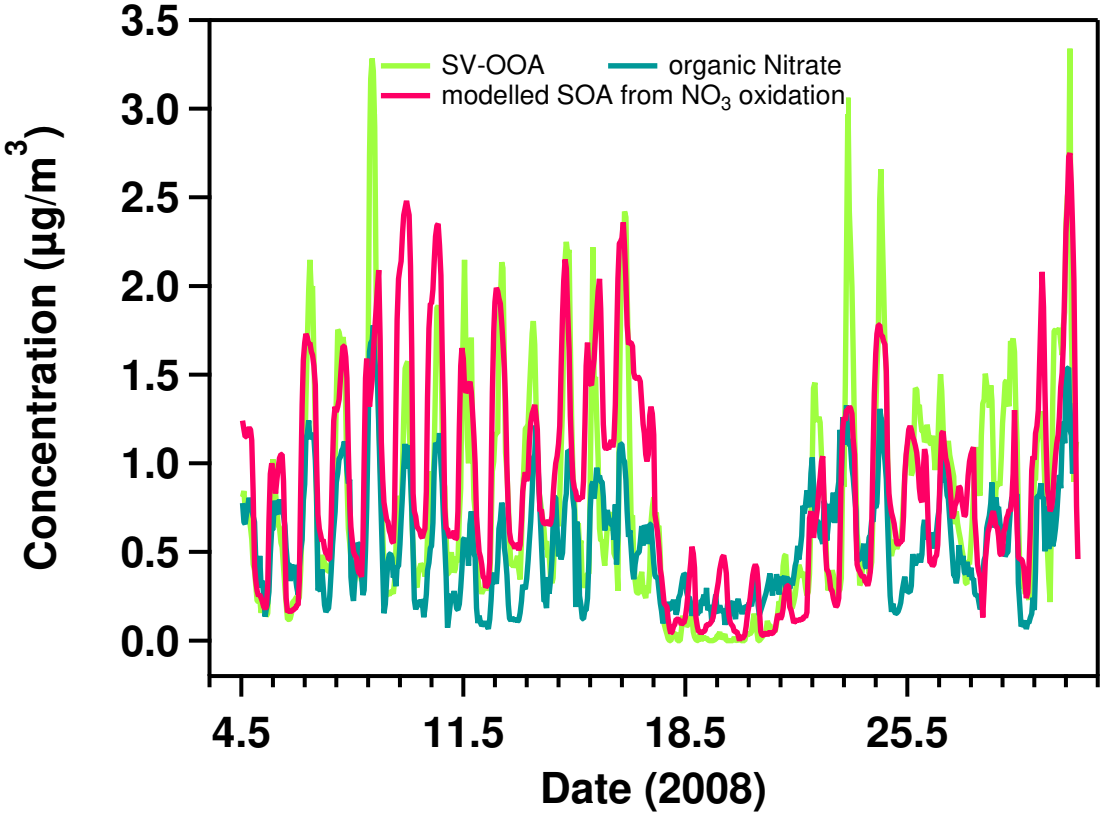
SV-OOA
organic Nitrate
modelled SOA from NO_3 oxidation
Concentration (µg/m^3)
3.5
3.0
2.5
2.0
1.5
1.0
0.5
0.0
4.5
11.5
18.5
25.5
Date (2008)

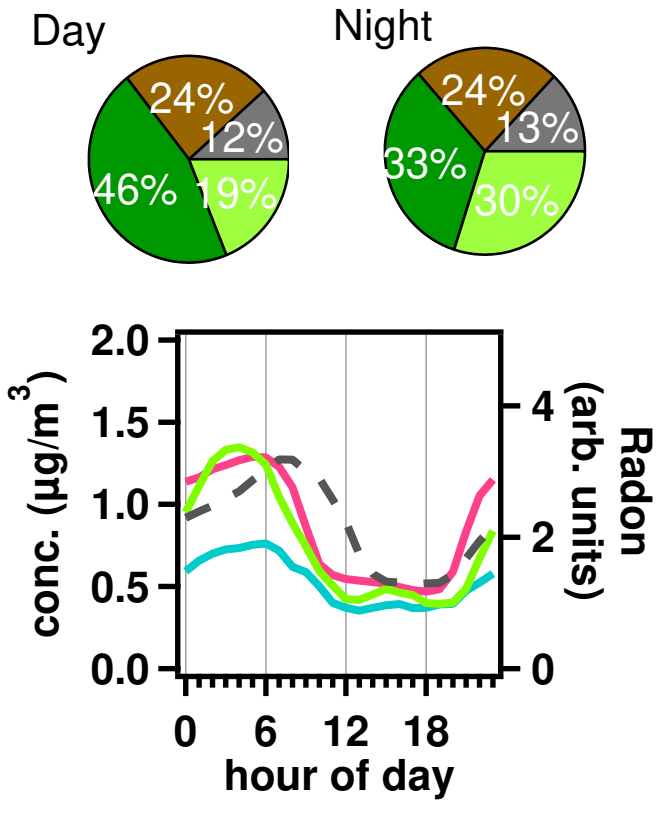
Day
Night
24%
12%
46%
19%
24%
13%
33%
30%
conc. (µg/m^3)
Radon (arb. units)
2.0
1.5
1.0
0.5
0.0
4
2
0
0
6
12
18
hour of day

Figure 3. Figure

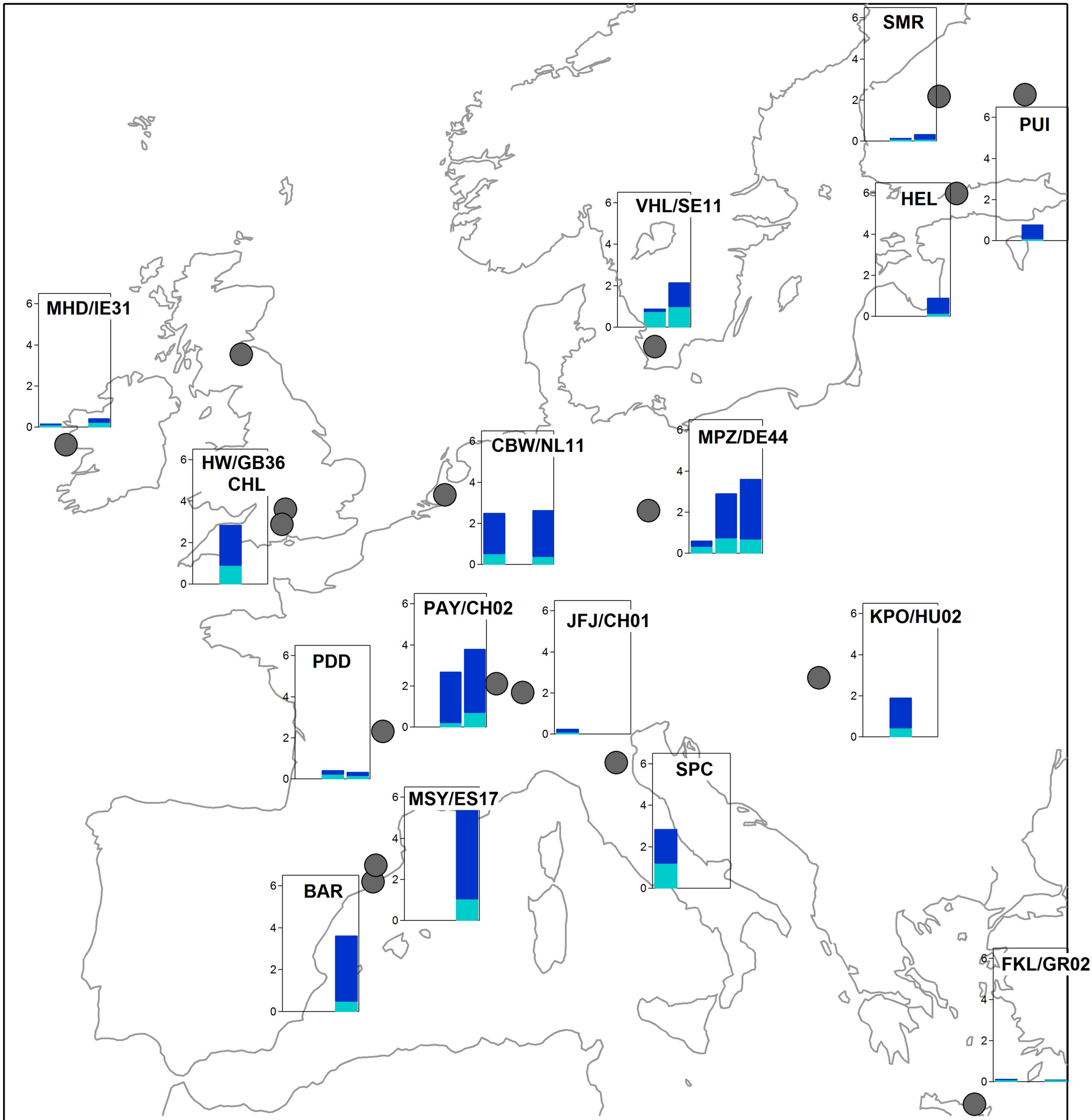
SMR
PUI
HEL
VHL/SE11
MHD/IE31
HW/GB36
CHL
CBW/NL11
MPZ/DE44
PAY/CH02
JFJ/CH01
KPO/HU02
PDD
SPC
MSY/ES17
BAR
FKL/GR02

Figure 4. Figure

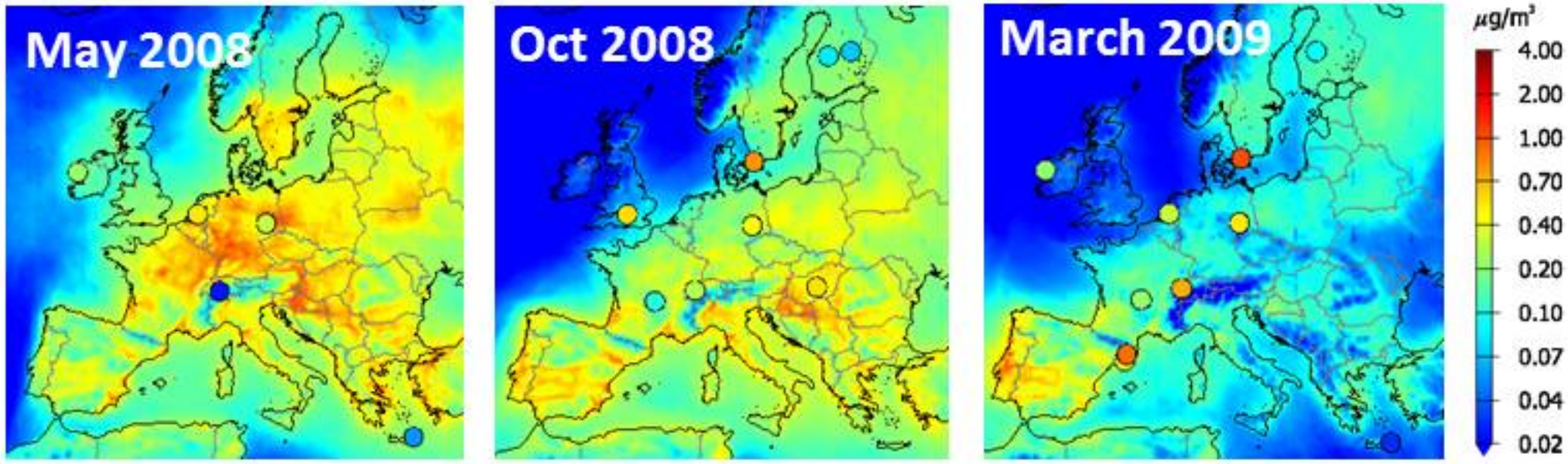
May 2008
Oct 2008
March 2009
µg/m³
4.00
2.00
1.00
0.70
0.40
0.20
0.10
0.07
0.04
0.02